

Preparation and Characterization of Ti^{3+} & Cr^{3+} : Li_2O - LiF - B_2O_3 - ZnO Optical Glasses

L. Vijayalakshmi^{*}, V. Naresh, R. Ramaraghavulu, B.H. Rudramadevi and S. Buddhudu

Department of Physics, Sri Venkateswara University, Tirupati 517 502, India.

ABSTRACT

A transparent base glass in the chemical composition Li_2O - LiF - B_2O_3 - ZnO (LBZ) has successfully been prepared also a couple of transition metal (Ti^{3+} & Cr^{3+}) ions doped into this glass matrix have also been done for their further analysis. Structural (XRD, FTIR & Raman) and thermal (TG-DTA) properties and also absorption spectrum of LBZ glass have been analyzed. Optical absorption, photoluminescence (excitation & emission) spectra of Ti^{3+} & Cr^{3+} : Li_2O - LiF - B_2O_3 - ZnO and their spectral assignments, dielectric (ϵ' & $\tan\delta$) and conductivities (σ_{ac} & σ_{dc}) have also been undertaken. The XRD profile of the host glass confirms its amorphous nature. Weight loss in the precursor sample powder, glass transition temperature (T_g) and crystalline temperature (T_c) have been identified from the TG-DTA profiles. FTIR and Raman spectra of the host glass show vibrational bands of B-O from $[BO_3]$ and $[BO_4]$ units and Li-O. The absorption spectrum of Cr^{3+} : LBZ glass has shown two bands at 412 nm (${}^4A_{2g}(F) \rightarrow {}^4T_{1g}(F)$) and 579 nm (${}^4A_{2g}(F) \rightarrow {}^4T_{2g}(F)$). In respect of Ti^{3+} : LBZ glass, only one broad band at 490 nm (${}^2B_{2g} \rightarrow {}^2B_{1g}$) has been measured. From the optical absorption spectral positions, their crystal field (Dq) and the Racah (B & C) interaction parameters have been evaluated. Dielectric constant and losses (ϵ' and $\tan\delta$) of all three glasses have been studied in the frequency range from 1Hz to 1M Hz at room temperature and computed conductivities (σ_{ac} and σ_{dc}).

Keywords: Cr^{3+} & Ti^{3+} glasses and Dielectric analysis.

I. INTRODUCTION

Over the past few years, a great deal of interest has been focused towards the development of glassy materials containing different transition metal ions for various applications [1-4]. Amongst a wide variety glass systems, particularly, borate (B_2O_3) based system has become popular, keeping in view its glass nature, transparency, several other physical and chemical properties associated with its thermal stability, it is considered here by us, to undertake our present investigation here. In this direction of work, we have primarily developed dual component glass (B_2O_3 - Li_2O), it has come up well, this has motivated us to further add to this dual system with two more salts like LiF and ZnO for further betterment and improvisation of UV transmission ability and also transparency as well with good stability in them. To the basic glass network former B_2O_3 , addition of an intermediate salt Li_2O causes an increase in the conductivity of the glass. Further, it is interesting to mention that addition of modifier salt LiF enhances the UV transmission ability and ZnO improves the thermal stability with good chemical durability [4]. These glasses are found to be resisting the atmospheric moisture and are readily accept good amount of dopant transition metal or rare earths in those matrices in an ease. Addition of alkali oxides modify the boroxol rings, forming complex borate

groups during transform from three- coordinated to four- coordinated boron atomic nature [5-9].

Amongst different transitional metal ions, Cr^{3+} and Ti^{3+} are popularly known as lasing ions, this has prompted us to undertake these two ions as dopant ions in the chosen multi-component glass (LBZ) matrix to study their optical and conductivity properties.

II. EXPERIMENTAL STUDIES

2.1 Glass samples preparation

Glasses studied in the present work were prepared by a standard melt quenching technique. The chemical compositions (all are in mol %) of the host glass with and without transition metal ions as dopants are as follows:

- (i) 30 Li_2O -20 LiF -45 B_2O_3 -5 ZnO (LBZ) glass
- (ii) (0.5 mol%) TiO_2 :30 Li_2O -20 LiF -44.5 B_2O_3 -5 ZnO (Ti^{3+} : LBZ) glass
- (iii) (0.5 mol %) Cr_2O_3 :30 Li_2O -20 LiF -44.5 B_2O_3 -5 ZnO (Cr^{3+} : LBZ) glass

The starting chemicals were used in analytical grade such as H_3BO_3 , Li_2CO_3 , LiF, $ZnCO_3$, TiO_2 and Cr_2O_3 . All the chemicals were weighed in 10g batch each separately, thoroughly mixed and finely powdered using an agate mortar and pestle and each of those was collected into a porcelain crucible and heated gradually in an electric furnace for melting

them for an hour at 950°C. These melts were quenched in between two smooth surfaced brass plates to obtain glasses in circular designs with 2-3 cm in diameter and with a thickness of 0.3 cm. Thus, obtained glass samples are used in the present work analysis.

2.2 Measurements

XRD profiles were recorded on a Seifert X-ray diffractometer (model 3003TT) with CuK_α radiation ($\lambda = 1.5406 \text{ \AA}$) at 40 KV and 20 mA with a Si detector and $2\theta = 10^\circ$ and 60° at the rate of $2^\circ/\text{min}$. A simultaneous measurement of TGA and DTA was carried out on NetZsch STA 409 at a heating rate of $10^\circ\text{C}/\text{min}$ with N_2 as the purging gas was obtained to correlate the results for a better understanding of the trends. FTIR spectrum of the sample was recorded on a Nicolet -5700 FT-IR spectrometer using KBr pellet technique in the range of $4000\text{-}400 \text{ cm}^{-1}$. Raman spectrum was measured using Jobin Yvon Horiba (LABRAM HR - 800) Micro-Raman Spectrometer attached with a He-Ne /Nd-YAG lasers as the excitation sources, having an output power of 15 mW with a laser beam spot size as $100 \mu\text{m}$ by employing an appropriate lens system. Electrical conductivity measurements were carried at room temperature over a frequency range of 1 Hz – 1 MHz at ac voltage strength of $0.5 V_{\text{rms}}$ on a Phase Sensitive Multimeter (PSM 1700) in LCR mode. Absorption spectra of glasses were measured on a Varian-Cary-Win Spectrometer (JASCO V-570). The emission spectra of Cr^{3+} and Ti^{3+} doped glasses were measured in a steady state mode on a SPEX Fluorolog-3(Model-II) Fluorimeter.

III. RESULTS AND DISCUSSION

3.1 XRD spectrum

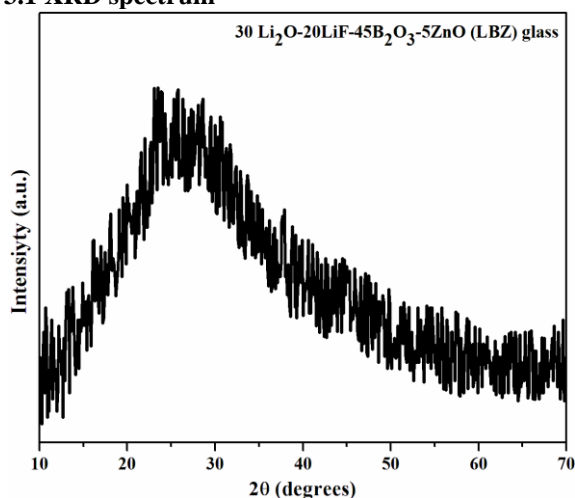


Fig.1: XRD profile of the host $\text{Li}_2\text{O-LiF-B}_2\text{O}_3\text{-ZnO}$ (LBZ) glass.

In Fig.1, XRD profile of $\text{Li}_2\text{O-LiF-B}_2\text{O}_3\text{-ZnO}$ (LBZ) glass has been shown with a broad hollow

band (diffused peak) at 2θ ($20^\circ - 30^\circ$), which clearly indicates glass amorphous nature. Similar nature has been observed in the case of transition metal ions containing LBZ glasses.

3.2 Thermal (TG-DTA) analysis

TG-DTA profiles are simultaneously measured for the $\text{Li}_2\text{O-LiF-B}_2\text{O}_3\text{-ZnO}$ (LBZ) precursor chemical mix as shown in Fig.2.

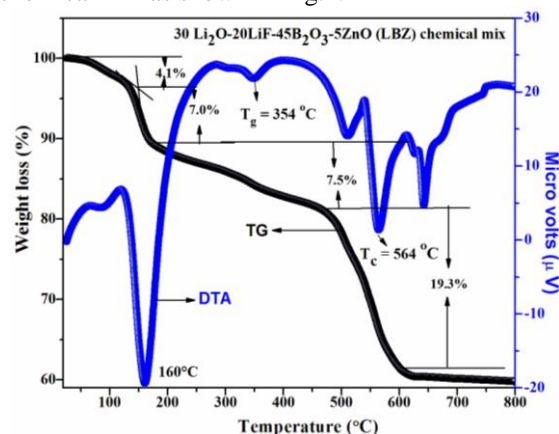


Fig.2: TG-DTA profiles of the host $\text{Li}_2\text{O-LiF-B}_2\text{O}_3\text{-ZnO}$ (LBZ) precursor chemical mix

TG profile displays that the weight loss of the sample takes place in a multistep process in the temperature range of $39^\circ\text{C}-700^\circ\text{C}$. The initial weight loss of sample occurs between 39°C and 135°C due to the decomposition of the organic compounds that were used during the grinding of chemicals mix, the observed weight has been at 4.1%. The second weight loss has been noticed in the temperature range of $135^\circ\text{C} - 177^\circ\text{C}$, due to the transformation of boric acid (H_3BO_3) at 135°C into meta-boric acid (HBO_2), which crystallizes in three different forms: $\alpha\text{-HBO}_2$ (orthorhombic), $\beta\text{-HBO}_2$ (monoclinic), and $\gamma\text{-HBO}_2$ (cubic). Among them, the cubic ($\gamma\text{-HBO}_2$) phase is reported to be more stable; with a weight loss of 7.0%. Upon further heating, the third weight loss has been noticed in the temperature range of $177^\circ\text{C} - 462^\circ\text{C}$ because of the conversion of HBO_2 as tetraboric acid or pyroboric acid, which in turn becomes as anhydrous oxide as boron trioxide (B_2O_3) in crystalline form that melts at 462°C , the weight loss there has been at 7.5%. The final weight loss in the temperature range $460^\circ\text{C}-595^\circ\text{C}$ due to decomposition of Li_2CO_3 into Li_2O and CO_2 with a weight loss of 19.3%. There exists no significant weight loss beyond 600°C as is seen from the TG profile pertaining to the glass related precursor chemicals mixture [10]. From DTA profile, glass transition temperature (T_g) is identified at 351°C and two sharp exothermic peaks have also been observed at 160°C and 564°C respectively. The peak at 160°C is attributed to a short range order and partial melting of small percentage of impurity phase & change in

phase, the other peak at 564°C is due to the heat loss during the crystallization, which is the peak at the crystallization temperature (T_c).

3.3 FTIR Spectral Analysis

The FTIR spectrum of $\text{Li}_2\text{O-LiF-B}_2\text{O}_3\text{-ZnO}$ (LBZ) glass has been shown in Fig.3, revealing characteristic peaks that are located at 556 cm^{-1} , 726 cm^{-1} , 1028 cm^{-1} , 1236 cm^{-1} , 1399 cm^{-1} , 1596 cm^{-1} , 2850 cm^{-1} , 2931 cm^{-1} , 3440 cm^{-1} & 3793 cm^{-1} .

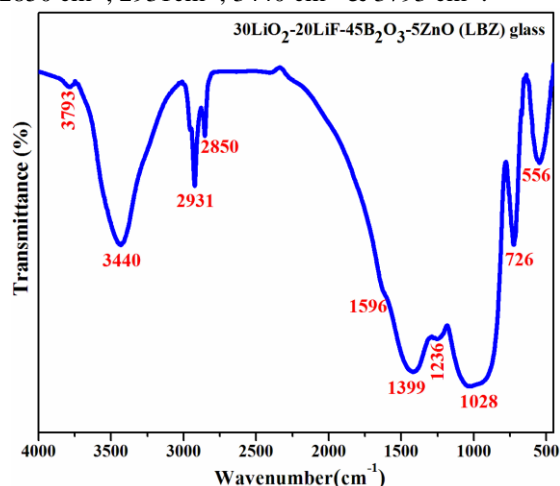


Fig.3: FTIR spectrum of host $\text{Li}_2\text{O-LiF-B}_2\text{O}_3\text{-ZnO}$ (LBZ) glass.

The broad bands are due to combination of factors such as high degeneracy of vibrational state, thermal broadening of lattice dispersion band and mechanical scattering from the sample. The band arising at 726 cm^{-1} is due to bending vibrations of B-O in BO_4 units from tri-, tetra-, and penta borate groups. Pure B_2O_3 contains only three coordinated boron atoms, but when Li^+ ions are added, some of these ions are transformed into four coordinated tetrahedral, creating some non-bridging oxygens. The band at 1028 cm^{-1} is attributed to such BO_4 units [5, 11]. The band at 1236 cm^{-1} is attributed to the asymmetric stretching vibrations of O-B bonds from ortho borate groups. The band at 1236 cm^{-1} indicates the presence of BO_3 unit with non-bridging oxygen existing in boron oxygen network. The band at 1399 cm^{-1} is due to the stretching of B-O bonds of various borate arrangements containing planar six membered borate groups, exhibiting a compositional dependence suggestive of overlapping bands originating from different species, the peak at 1596 cm^{-1} is raised from B-O stretching vibrations of $[\text{BO}_3]^{3-}$ units. The band at 2850 cm^{-1} can be attributed to hydrogen bonds and a broad band at 3440 cm^{-1} could be attributed to the hydroxyl group (due to stretching of OH^-) in the present glass network formed at non-bridging oxygen site. The contribution due to borate network dynamics is mostly in the mid-infrared region of the profile, where as for lithium cation motion dominates

in the low frequency region. The information obtained from FTIR spectra of these glasses address the existence of interactions between the alkali metal ions and the borate glass network and this in turn helps to understand the ionic transport phenomena of these glasses [5, 12].

3.4 Raman Spectral Analysis

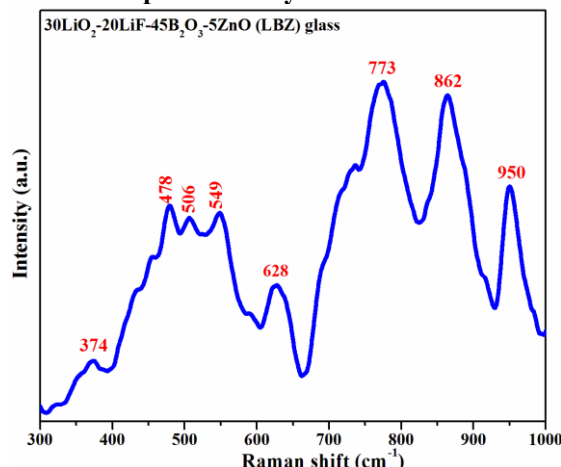


Fig.4: Raman spectrum of host $\text{Li}_2\text{O-LiF-B}_2\text{O}_3\text{-ZnO}$ (LBZ) glass.

Fig.4 shows Raman spectrum of $\text{Li}_2\text{O-LiF-B}_2\text{O}_3\text{-ZnO}$ (LBZ) glass exhibiting bands at 374 cm^{-1} , 478 cm^{-1} , 506 cm^{-1} , 549 cm^{-1} , 628 cm^{-1} , 773 cm^{-1} , 862 cm^{-1} , 950 cm^{-1} and 983 cm^{-1} . In literature it is reported that, pure B_2O_3 exhibits a strong band at 806 cm^{-1} and which is assigned to the boroxol ring oxygen breathing vibrations involving a very little boron motion [13, 14]. In this LBZ glass with the presence of Li_2O , the B_2O_3 transforms into a complex network which involves a boroxyl ring coupled with four fold coordinated boron (BO_4) because of non bridging oxygens. The peak at 773 cm^{-1} is assigned to breathing vibrations of a six member rings with BO_3 triangles replaced by BO_4 tetrahedral units [15]. A band at 549 cm^{-1} is due to bending mode (B-O-B) of BO_3^{3-} units. The peaks at 950 cm^{-1} and 983 cm^{-1} are due diborate group [16]. In the lower frequency range, a peak is observed at 374 cm^{-1} due to librational mode of BO_3 and BO_4 units.

3.5 Absorption and Photoluminescence Spectral Analysis

The optical absorption spectra of host LBZ; Ti^{3+} :LBZ and Cr^{3+} :LBZ glasses are shown in Figs.5(a, b & c). Absorption spectrum of host $\text{Li}_2\text{O-LiF-B}_2\text{O}_3\text{-ZnO}$ (LBZ) glass shown in Fig.5(a) exhibits good transparency with its absorption edge lying in UV region (UV-transmission ability). In Fig.5(b), absorption spectrum of Ti^{3+} :LBZ glass has been revealing a broad band centered at 490 nm covering the range from 460 nm to 580 nm that is assigned to the electronic transitions of ${}^2\text{B}_{2g} \rightarrow {}^2\text{B}_{1g}$ due to Ti^{3+}

ions located at distorted octahedral position [17-20]. From the observed electronic transition the ligand field parameter Dq is computed to be at 2040.81cm^{-1} which is in good agreement with reported values (2050cm^{-1}) in literature [20]. ΔE , B and C could not be calculated because Ti doped glass exhibits only one broader peak.

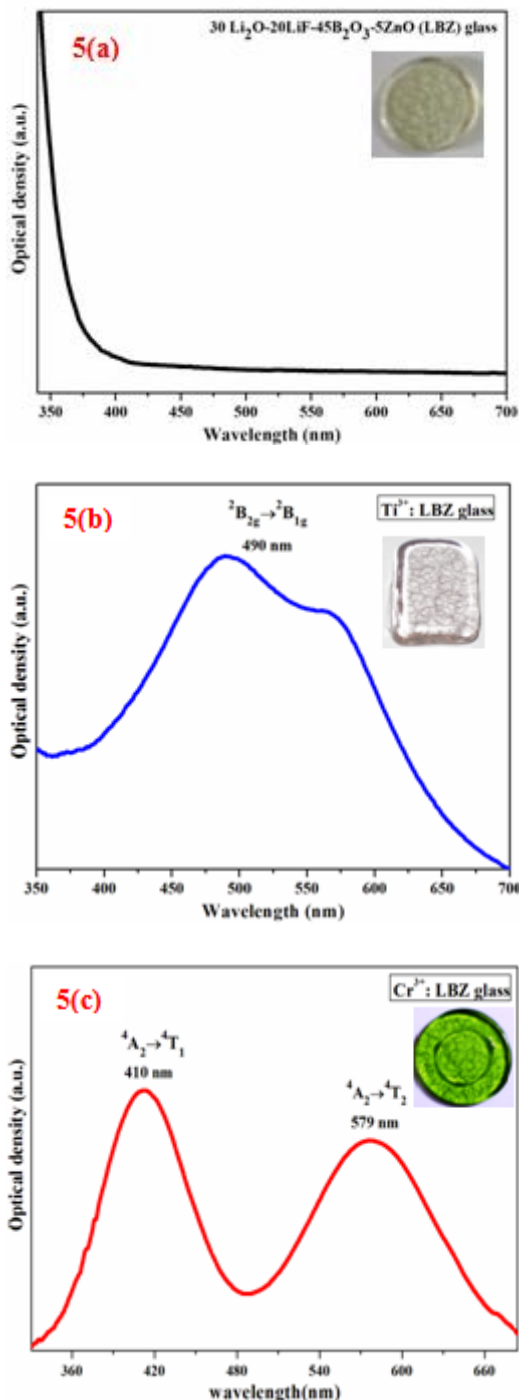


Fig.5: Absorption spectra of (a) host LBZ (b) Ti³⁺: LBZ and (c) Cr³⁺: LBZ glasses.

In Fig.5(c) optical absorption spectrum of Cr³⁺: LBZ has been shown with two broad bands of Cr³⁺

ions in octahedral symmetry at 412 nm, 579 nm and a weak band at 670 nm assigned to the spin allowed optical d-d transitions of ${}^4A_{2g}(F) \rightarrow {}^4T_{1g}(F)$, ${}^4A_{2g}(F) \rightarrow {}^4T_{2g}(F)$ and a spin forbidden transition of ${}^4A_{2g}(F) \rightarrow {}^2T_{1g}(G)$ respectively [21, 22]. From the observed electronic transitions, the crystal field ($10Dq$) and Racah (B & C) parameters have been calculated [23, 24]. The crystal field strength (Dq) parameter gives an energy difference between the ground state first excited state of Cr³⁺, ${}^4A_{2g}$ and ${}^4T_{2g}$ respectively, and the equation is of the form:

$$10Dq = E({}^4A_{2g} \rightarrow {}^4T_{2g}) \quad \dots (1)$$

ΔE is the energy difference between two peaks of Cr³⁺, at ${}^4T_{1g}$ and ${}^4T_{2g}$ respectively, and the equation is given by:

$$\Delta E = E({}^4T_{1g}) - E({}^4T_{2g}) \quad \dots (2)$$

The Racah parameter B (electrostatic parameter which is a measure of the inter-electronic repulsion) is calculated from the following formula:

$$\frac{B}{Dq} = \frac{\left(\frac{\Delta E}{Dq}\right)^2 - 10\left(\frac{\Delta E}{Dq}\right)}{15\left[\left(\frac{\Delta E}{Dq}\right) - 8\right]} \quad \dots (3)$$

The energy of the ${}^4T_{2g}$ depends on the Dq and B, the Dq value calculated for ${}^4A_{2g} \rightarrow {}^4T_{2g}$ transition from eq. (1) is 1727.11cm^{-1} and the energy difference ΔE from eq (2) is found to be at 7000.69cm^{-1} . Substituting the obtained values of Dq and ΔE in the eq (3), B is evaluated to be 703.2cm^{-1} . The value of C is evaluated from the equation given below:

$$C = \frac{\left[E(^2E) - 7.9B + 1.8B^2/Dq\right]}{3.05} \quad \dots (4)$$

Here $E(^2E) = 14044.9\text{cm}^{-1}$ is taken from the earlier reports [24]. Using the values of Dq , ΔE and B, the value of C is given by 2952.4cm^{-1} . The value of 703.2cm^{-1} obtained for Racah parameter, B is 76% that of free ion value (918cm^{-1}) indicating a considerable orbital overlap with a strong covalent metal-ligand band. However, the value of $Dq/B \ll 2.3$, then Cr³⁺ ions lies in weak crystal field sites or else if $Dq/B \gg 2.3$, then Cr³⁺ ions lies in strong crystal field sites and for intermediated crystal field sites $Dq/B \approx 2.3$. In this glass system the value of $Dq/B = 2.45 > 2.3$, implies that Cr³⁺ ions lies in strong crystal field sites.

Fig.6(a & b) show excitation and emission spectral profiles of Ti³⁺:LBZ glass. From the excitation spectrum, two excitation bands are found at 260 nm and 373 nm respectively. A broad absorption band at 260 nm is attributed to the charge

transfer band of $Ti^{3+} - O^-$ (exists in the intervals of network) and $O^{2-} - Ti^{4+}$ (exists as network forming ions to compose network) ions owing to the co-existence of both the ions in the glass matrix [25].

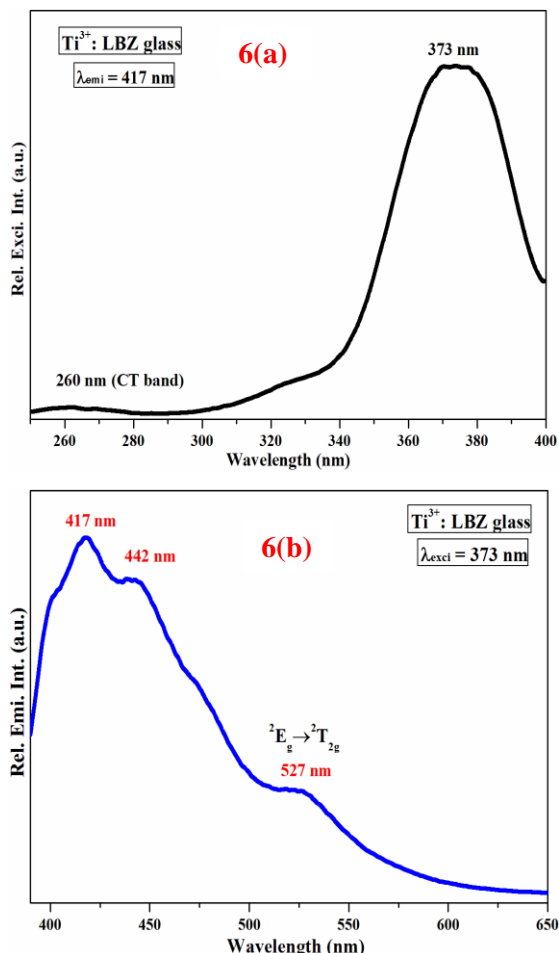


Fig.6: (a) Excitation and (b) emission spectra of Ti^{3+} : LBZ glass.

The UV absorption band around 260 nm could be related to charge transfer transition between Ti^{4+} and O^{2-} ions [26]. The band at 373 nm has been used to measure the emission spectra of Ti^{3+} : LBZ glass. The emission spectrum has bands at 417 nm & 442 nm in blue region due to the charge transfer band between O^- and Ti^{3+} and 527 nm in green region assigned to the transition ${}^2E_g \rightarrow {}^2T_{2g}$, which confirms the presence of titanium ion in Ti^{3+} : LBZ glass [25-27].

The excitation spectrum of Cr^{3+} :LBZ glass has been shown in Fig.7(a) with a couple of bands at 416 nm and 474 nm, of these two, prominent band being at 474 nm, it has been used in the measurement of emission spectrum of Cr^{3+} glass. In Fig. 7(b), emission spectrum of Cr^{3+} : LBZ glass depicting two emission bands at 517nm and 529 nm (yellowish green region) and 554 nm (green region) assigned to

the transitions of ${}^4D_{7/2} \rightarrow {}^6S_{5/2}$ and ${}^4D_{1/2} \rightarrow {}^6S_{5/2}$ respectively.

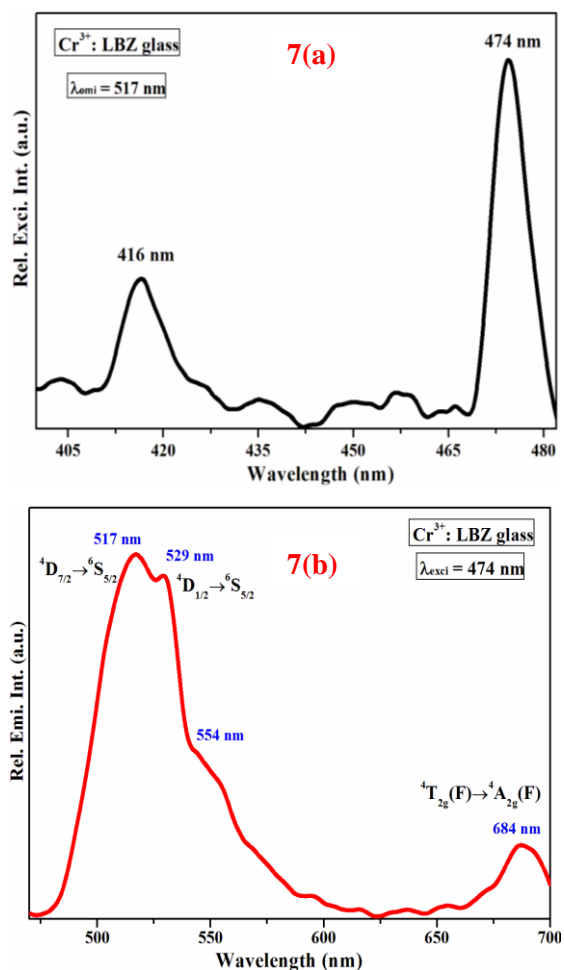


Fig.7: (a) Excitation and (b) emission spectra of Cr^{3+} : LBZ glass.

The band at 684 nm is assigned to the electronic transition of ${}^4T_{2g}(F) \rightarrow {}^4A_{2g}(F)$ confirming its Cr^{3+} state [28, 29].

3.6 Dielectric and Conductivity Properties

Dielectric properties of ionic conducting glasses are due to the contribution of electronic, ionic, dipole orientations and space charge polarizations; out of this space charge polarization depends upon the nature of the glass. The charge carriers in a glass cannot move freely through the glass but those could be displaced and thus become polarized depending upon applied alternating field. The complex permittivity of the glass system is determined by using the impedance data:

$$\epsilon^* = \frac{1}{(j\omega C_o Z^*)} = \epsilon' - j\epsilon'' \quad \dots (6)$$

Where Z^* is the complex impedance, C_o is the capacitance of free medium. The real part of

permittivity (dielectric constant) ϵ' represents the polarizability of the material, while the imaginary part (dielectric loss) ϵ'' represents the energy loss due to polarization and ionic conduction. The dielectric parameters (dielectric constant (ϵ'), dielectric loss tangent ($\tan\delta$)) and ac σ_{ac} conductivities are calculated using the formulae [30]:

$$\epsilon' = \frac{Cd}{\epsilon_0 A} \quad \dots (7)$$

$$\tan\delta = \frac{\epsilon''}{\epsilon'} \quad \dots (8)$$

$$\sigma_{ac} = \omega\epsilon_0\epsilon'' \quad \dots (9)$$

Where C is the capacitance of the glass sample, ϵ_0 is the permittivity of the free space (8.85×10^{-12} F/m and A is the cross-sectional area of electrode.

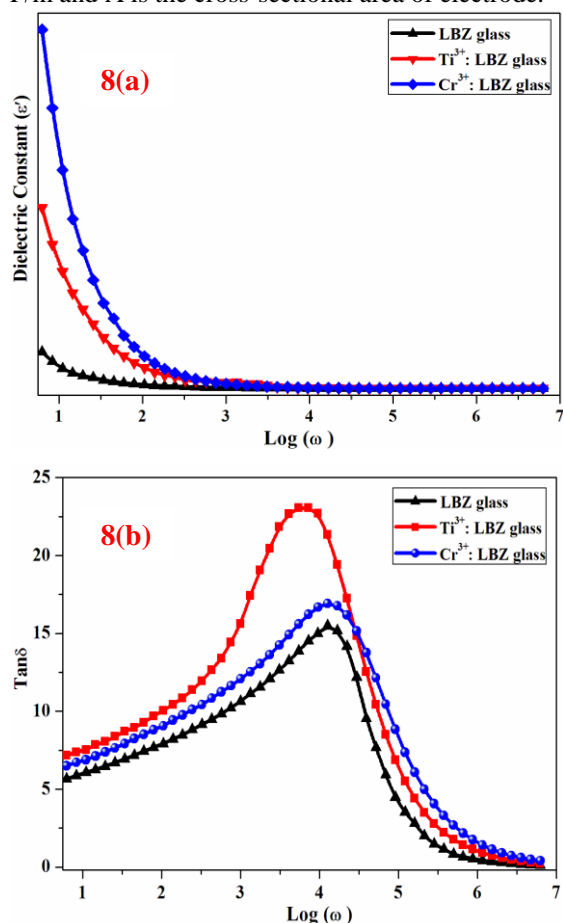


Fig.8: (a) Dielectric constant and (b) dielectric loss as a function of $\log(\omega)$ at room temperature for host LBZ, Ti^{3+} :LBZ and Cr^{3+} :LBZ glasses.

Fig.8(a) shows the dependence of dielectric constant (ϵ') as a function of frequency at room temperature for host (LBZ), Ti^{3+} :LBZ and Cr^{3+} :LBZ glasses. The profiles of all three studied glasses have exhibited same trend having high dielectric constant value at lower frequencies followed by decrease and

attains constant value as the applied field increases up to 1 MHz. Such a trend could be due to accumulation of immobile charges at the electrode-electrolyte interface resulting in polarization at lower frequencies, while at higher frequencies, the periodic reversal of electric field at interface occurs so fast that no excess ion diffuses in the direction of electric field [30, 31].

The dielectric loss tangent ($\tan\delta$) is the phase difference due to the loss of energy within the sample. Variation of dielectric loss tangent ($\tan\delta$) as a function of frequency for host (LBZ), Ti^{3+} :LBZ and Cr^{3+} :LBZ glasses are shown in Fig.8(b). From profiles it is observed that dielectric loss of the three studied glass systems decrease with an increase in frequency due to mobility of conducting species with a relaxation peak around 10 kHz. The relaxation peaks are asymmetric in nature. Such trend is attributed to thermally activated relaxation of freely rotating dipoles trying to align themselves in the applied field direction or in other words motion of space charges gives rise to such loss peaks [32].

The frequency ($\log\omega$) dependent ac conductivity ($\log\sigma_{ac}$) profiles for host (LBZ), Ti^{3+} :LBZ and Cr^{3+} :LBZ are shown in Fig. 9 are analyzed on the basis of Jonscher universal power law [33]:

$$\sigma(\omega) = \sigma_{dc} + A\omega^s \quad 0 < s < 1 \quad \dots (10)$$

Where σ_{dc} is the dc conductivity of the samples, A is temperature dependent constant, $\omega = 2\pi f$ is the angular frequency of the applied field and s is the power law exponent in the range $0 < s < 1$, represents the degree of interaction between the mobile ions. The frequency dependence of conductivity is sum of the dc conductivity due to movements of free charges and polarization conductivity (ac conductivity) due to movements of bound charges.

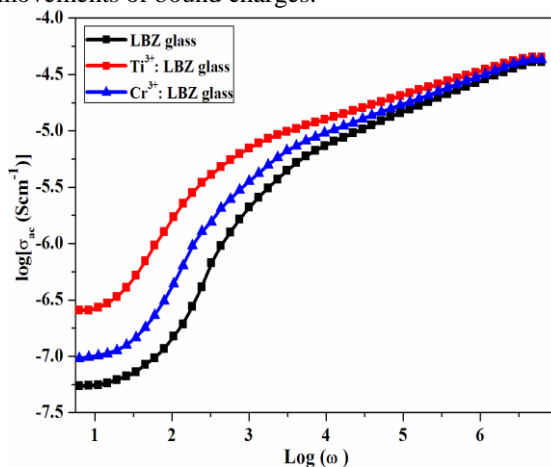


Fig.9: Conductivities ($\log\sigma_{ac}$) as a function of $\log(\omega)$ at room temperature for (a) host LBZ (b) Ti^{3+} :LBZ and (c) Cr^{3+} :LBZ glasses.

In Fig.9 profiles of frequency dependence of ac conductivity have been shown, it is observed that, the glass system with and without TiO₂ and Cr₂O₃ as dopant ions exhibit same trend of increasing in ac conductivity as a function of frequency. It is also observed that in the low frequency region, ion conductivity is low and frequency independent, which could be attributed to the polarization effects at the electrode-electrolyte interface and charge carriers having high relaxation time due to high energy barrier respond less in low frequency region. In the high frequency region, more number of charge carriers is availability for conduction due to low energy barrier and they respond easily. Hence, these glasses exhibit high conductivity at high frequencies. It is also observed that curves were tending to merge into a single curve becoming strongly frequency dependent at higher frequencies [30-33]. These curves show almost a linear behavior which follows a power law relation in the higher frequency region:

$$\sigma(\omega) = A\omega^s \quad s < 1 \quad \dots (11)$$

The exponent *s* can be measured by taking slope of log σ_{ac} versus log ω for the curves from the

$$\text{equation } S = \frac{d(\text{Ln}\sigma_{ac}(f))}{d(\text{Ln}(f))}, \text{ found to lies in the}$$

range of 0.7 to 0.9 which explains the interaction between the mobile ions.

Fig. 10 shows the complex impedance spectrum at room temperature in the frequency range 1Hz - 1M Hz for host (LBZ), Ti³⁺:LBZ and Cr³⁺:LBZ glass.

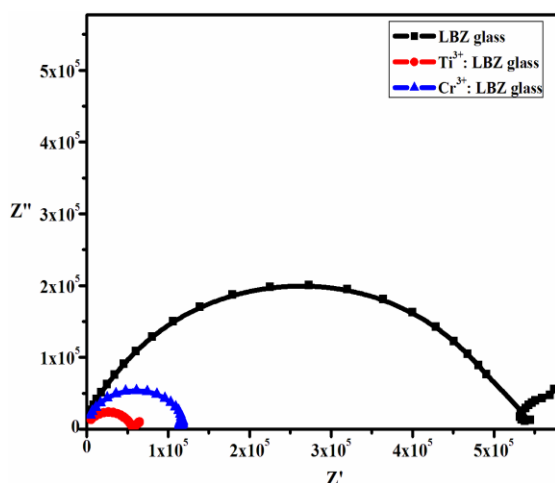


Fig 10: Complex impedance plots (Nyquist plots) as a function of log (ω) at room temperature for (a) host LBZ (b) Ti³⁺:LBZ and (c) Cr³⁺:LBZ glasses.

All the studied glasses exhibited same trend of single semi circular arc with its centre on the Z'- axis, beginning from the origin at higher frequencies and ends at lower frequencies on Z'- axis. The

intersection of the semicircle with the Z'- axis at lower frequencies is considered as the sample bulk resistance (R_b).The diameter of the semicircle drawn through the centre from the origin makes an angle $\sim\pi/2$ with the Z'- axis. The bulk conductivity for the glass samples are calculated from the relation [34, 35]:

$$\sigma_{dc} = \frac{L}{R_b A} \quad \dots (12)$$

Where ' σ_{dc} ' is bulk conductivity, 'L' is the thickness of the glass sample, 'R_b' is the bulk resistance, 'A' is the effective area of the host glass studied. The ac- and dc-conductivity values of the three studied glasses are given in Table 1.

Table. 1:

σ_{ac} & σ_{dc} - conductivity values of host LBZ, Ti³⁺:LBZ and Cr³⁺:LBZ glasses

| Glass | ac conductivity (S cm ⁻¹) | dc conductivity (S cm ⁻¹) |
|-----------------------|---------------------------------------|---------------------------------------|
| LBZ | 7.28x 10 ⁻⁷ | 3.49x 10 ⁻⁷ |
| Ti ³⁺ :LBZ | 1.03 x 10 ⁻⁶ | 1.61 x 10 ⁻⁶ |
| Cr ³⁺ :LBZ | 1.65 x 10 ⁻⁶ | 2.44 x 10 ⁻⁶ |

IV. CONCLUSION

In summary, it is concluded that optical glasses in general chemical composition of 30Li₂O-20LiF-45 B₂O₃-5ZnO (host LBZ glass), 0.5mol% Cr₂O₃: 30Li₂O-20LiF-45.5B₂O₃-5ZnO (Cr³⁺: LBZ glass) & 0.5mol% TiO₂: 30Li₂O-20LiF-45.5B₂O₃-5ZnO (Ti³⁺: LBZ glass) have been prepared by a standard melt quenching procedure. XRD, FTIR, Raman analysis, thermal properties have been studied for the host LBZ glass, while optical absorption, photoluminescence (excitation & emission), dielectric and conductivity properties have been studied for Ti³⁺ and Cr³⁺ doped glasses. The amorphous nature of the glass has been confirmed from its XRD profile. Both FTIR and Raman spectra of the host LBZ glass have also been analyzed. Thermal decomposition in the precursor chemical mix has been understood from its TG profile and glass transition temperature 351°C and crystalline temperature 510°C have been found suitably from its DTA profile. Based on the optical absorption spectra of Ti³⁺:LBZ and Cr³⁺:LBZ glasses, crystal field strength (Dq) and Racah parameters (B & C) are evaluated towards understanding of the nature of local symmetry and structural information on the neighboring atoms of dopant (Ti³⁺ & Cr³⁺) ions. The dielectric properties (ϵ' & $\tan\delta$), of these glasses are found to be decreasing with an increase in frequency due to an effect of polarization. With the addition of transition metal ions (Ti³⁺ & Cr³⁺), glasses containing those ions could reveal that their ac (σ_{ac} & σ_{dc}) conductivities are found to be enhanced when

compared with the host (LBZ) glass. Thus, we suggest that the present study has enabled us to take up further extension work on these glasses with several other transition metal ions as dopant ions and also certain rare earth ions too later on, to evaluate their optical, dielectric and conductivity performances for their applications appropriately.

REFERENCES

- [1] S.M. Kaczmarek, *Li₂B₄O₇ glasses doped with Cr, Cu, Eu & Dy*, *Opt. Mater.*, **19** (2002)189 -194.
- [2] A. Srinivasa Rao, J. Lakshmana Rao, R. Ramakrishna Reddy, T.V.Ramakrishna Rao, *Electron Paramagnetic Resonance and Optical absorption spectra of Cr(III) ions in alkali cadmium borosulphate glasses*, *Opt Mater.*, **4** (1995) 717-721.
- [3] Shaweta Mohan, Kulwant Singh Thind, Gopi Sharma, Leif Gerward, *Spectroscopic investigations of Nd³⁺ doped fluoro-and chloro borate glasses*, *Spectrochimica Acta Part A*, **70** (2008) 1173-1179.
- [4] Kang III Cho, Sun Hwa Lee, Dong Wook Shin, Yang Kuk Sun, *Relationship between glass network structure and conductivity of Li₂O-B₂O₃-P₂O₅ Solid electrolyte*, *Electrochimica Acta*, **52** (2006) 1576-1581.
- [5] R. Balaji Rao, Rosario A. Gerhardt & N. Veeraiiah, *Spectroscopic characterization conductivity and relaxation anomalies in Li₂O-mgO-B₂O₃ glass system: Effect of Nickel ions*, *J. Phys. Chem. Solids* **69** (2008) 2813-2826.
- [6] Samir Y.Marzouk & Fatma H.Elbatl, *Ultraviolet-Visible absorption of gamma-irradiated transition metal ions doped in sodium meta phosphate glass. Nuclear instruments and methods in Physics Research B* **248** (2006) 90-102.
- [7] M. Obula Reddy & S.Buddhudu, *Structural, dielectric,thermal and optical properties of Ti³⁺ or Cr³⁺: PVA Polymer films*. *Ferroelectrics* **413** (2011) 123-141.
- [8] M. Casalboni, V. Ciafardone, G. Giuli, B. Izzi, E. Paris, & P. Proposito, *An optical study of silicate glass containing Cr³⁺ and Cr⁶⁺ ions*. *J. Phy. Condens Matter.*, **8** (1996) 9059.
- [9] R. Kripal & S. Pandey, *Single crystal EPR, optical absorption and superimposition model study ofCr³⁺doped ammonium di hydrogen phosphate*. *Spectr Chem. Acta Part A* **76** (2010) 62–70.
- [10] V. Naresh & S. Buddhudu, *Structural, thermal, dielectric and ac conductivity properties of lithium fluoro-borate optical glasses*, *Ceram. Int.* **38** (2012) 2325-2332.
- [11] A. Terczynska-Madej, K. Cholewa-Kowalska & M. Laczka, *Coordination and valence state of transition metal ions in alkali borate glasses*, *Opt.Mater.*, **33** (2011) 1984-1988.
- [12] B.V.R. Chowdari & Zhou Rong, *Study of the fluorinated lithium borate glasses*, *Solid state ionics* **78** (1995).
- [13] J. Krogh-Moe, *Interpretation of the infrared spectra of boron oxide and alkali borate glasses*, *Phy.Chem.Glasses* **6** (1965) 46.
- [14] F.L. Galneer, *Planar rings in glasses*, *Solid state.Commun.*,**44** (1982) 1037.
- [15] B.P. Dwivedi & B.N.Khanna, *Cation dependence of Raman scattering in alkali borate glasses*, *J.Phys.Chem.Solids.*, **56** (1995) 39-49.
- [16] W.L. Konijnendijk, *Structure of borosilicate glasses*, *Philips Res. Rep.Suppl.***1** (1975) 243.
- [17] Fatam H El-Batal, *UV-visible, infra red, Raman and ESR spectra of gamma-irradiated TiO₂-doped soda lime phosphate glasses*, *Indian. J. Pure & Appl. Phys.* **47** (2009) 631-642.
- [18] Liu Humin and Gan Fuxi, *Time resolved fluorescence spectra of titanium-containing fluorophosphates glass*, *J. Non-Cryst. Solids* **80** (1986) 422-428.
- [19] J. Schmidt, *ESR of Ti³⁺ and Cr³⁺ in AlCl₃ single crystal*, *Phys. Lett.* **28 A** (1986) 419-420.
- [20] Gan Fuxi and Liu Humin, *Spectroscopy of transition metal ions in inorganic glasses*, *J. Non-Cryst. Solids* **80** (1986) 20-33.
- [21] Xia Haiping, Wang Jinhao, Wang Hongyin, Zhang Jianli, Zhang Yuepin & Xu Tiefeng, *Optical spectroscopy and crystal field strength of Cr³⁺ in various solid matrixes*, *Rare Metals* **25** (2006) 51-57.
- [22] C. Parthasaradhi reddy, V. Naresh, R.Ramaraghavulu, B.H. Rudramadevi & S. Buddhudu, *Optical and dielectric properties of Cr³⁺ & Cu²⁺: P₂O₅-ZnO-LiF glasses*, *Int. J. Eng. Res. & Appl.* **4** (2014) 127-134.
- [23] S.S.Pedro, L.P. Sosman, R.B. Barthem, J.C.G. Tedesco, H. N. Bordallo, *Effects of Cr³⁺ concentration on the optical properties of Cs₂NaAlF₆ single crystals*, *J. Lumin.* **134** (2013) 100-106.
- [24] G. Wang, Y. Huang, L. Zhang, Z. Lin, G. Wang, *Growth and spectroscopic characteristics of Cr³⁺:KSc(Wo₄)₂ crystal*, *Opt. Mater.*,**34** (2012) 1120-1123.
- [25] Mu-Tsun Tsai, Yee-Shin Chang, You-Hsin Chou, Kai-Min Tsai, *Photoluminescence of titanium doped zinc spinel blue-emitting*

- nanophosphors, *J. Solid State Chem.* **214** (2014) 86-90.
- [26] L. Trikler, B. Berzina D. Jakimovica, J. Grabis, I. Steins, *Peculiarities of photoluminescence of Al₂O₃ bulk and nanosize powders at low temperatures*, *Opt. Mater.*, **33** (2011) 817-822.
- [27] G. Molnar, M. Benabdesselam, J. Borossay, D. Lapraz, P. Iacconi, V.S. Kortov & A.I. Surdo, *Photoluminescence and thermoluminescence of titanium ions in sapphire crystals*, *Radiation Measurements* **33** (2001) 663-667.
- [28] C.R. Kesavulu, R.P.S. Chakradar & J.L. Rao, EPR, optical, photoluminescence studies on Cr³⁺ ions in Li₂O-Cs₂O-B₂O₃ glasses- an evidence of mixed alkali effect, *J. Molecular Struct* **975** (2010) 93-99.
- [29] Wong Poh Sum, WanMing Hua, Eeu Tien Yew, Rosli Hssin and Zuhairi Ibrahim, *Photoluminescence Studies on Lithium – calcium Boro-Phosphate glasses doped with transition metal ions*, *Malaysian J. of Fundamental and Applied Sciences*, **8** (2012) 89-93.
- [30] V. Naresh and S. Buddhudu, *Studies on optical, dielectric and magnetic properties of Mn²⁺, Fe³⁺ & Co²⁺ Ions doped LFBCd Glasses*, *Ferroelectrics* **437** (2012) 110–125.
- [31] C.V. Chammal, J.P. Jog, *Dielectric relaxation in PVDF/BaTiO₃ nano composites*, *Express Polymer Letters* **2** (2008) 294-301.
- [32] E.M. Abdelrazek, I.S. Elashmawi, H.M. Ragab, *Manifestation of MnCl₂ fillers in corporate into the polymer matrices in their dielectric properties*, *Physica B* **403** (2008) 3097-3104.
- [33] K. Jonscher, *The ‘universal’ dielectric response*, *Nature* **267** (1977) 673-679.
- [34] N. Mir, M. Salavati-Niasari, *Effect of tertiary amines on the synthesis and photovoltaic properties of TiO₂ nanoparticles in dye sensitized solar cells*, *Electrochimica Acta* **102** (2013) 274-281.
- [35] Andrea Mogus-Milankovic, Kristina Skleplic, Hrvoje Blazanovic, PetrMosner, Maryna Vorokhta, Ladislav Koudelka, *Influence of germanium oxide addition on the electrical properties of Li₂O-B₂O₃-P₂O₅ glasses*, *J. Power Sources* **242** (2013) 91-98.